Electronic Supplementary Material (ESI) for Journal of Materials Chemistry A.

Supporting information

Porous Co-P foam as an efficient bifunctional electrocatalyst for hydrogen and oxygen evolution reaction

SeKwon Oh, HyoWon Kim, YongGuen Kwon, MinJoong Kim, EunAe Cho[*]*,*

HyukSang Kwon[*]

Dept. of Materials Science and Engineering, KAIST, Daejeon, 305-701, Republic of Korea.

Experimental Section

Preparation of Co-P foams and film by electrodeposition

Co-P foam and Co-P film were formed by electrodeposition using a three-electrode cell in an electrolyte composed of 0.1 M $CoSO_4$, 0.7 M H_2SO_4, 0.5 M $NaH_2PO_2.H_2O$ and 1.2 M $(NH4)_2SO_4$. A nodule-type copper sheet was used as substrate for the electrodeposition of Co-P foam. A pure Co plate and a standard calomel electrode (SCE) were used as counter and reference electrode, respectively. Co-P foams were deposited galvanostatically at cathodic current densities of 0.5, 1, 3, 5 and 9 A/cm^2 for 10 s in the prepared electrolytic solution with magnetic stirring. A Co-P film was electrodeposited at 50 mA/cm^2 for 300 s. All the electrodeposition processes were conducted at room temperature, 25 °C. The electrodeposited samples were dried in vacuum for 1 h after being rinsed with distilled water.

Characterization

To examine the effects of current density on the morphology of the prepared Co-P samples, surface images of the prepared Co-P samples were observed using a scanning electron microscope (SEM). Chemical composition of the Co-P samples was analyzed by EDS and XPS. Microstructure of the Co-P deposits was further investigated with a transmission electron microscopy (TEM). For the TEM analysis, the dried Co-P deposits were raked out from the substrate with tweezers, and then dispersed in ethanol with sonication for 30 min. Crystal structure of the Co-P deposits was identified by selected area electron diffraction (SAED) and by X-ray diffraction (XRD).

Electrochemical measurements

Electrochemical measurements were carried out in a three-electrode cell. A circular copper foil was pasted on a rotating disk glassy carbon electrode as working electrode. And a Pt wire

and SCE were used as counter electrode and reference electrode, respectively. HER activity was evaluated using a LSV test in 0.5 M H_2SO_4 and 1M KOH aqueous solution at a scan rate 1 mV/s. OER activity was also evaluated using a LSV test in 1 M KOH aqueous solution. All measured potentials were converted from SCE to reversible hydrogen electrode (RHE). In 0.5 M H_2SO_4, $E_{RHE} = 0.281V + E_{SCE}$, and in 1 M KOH, $E_{RHE} = 1.05\ V + E_{SCE}$.

Calculation of electrochemically active surface area

Electrochemically active surface area (ECSA) was evaluated from the following equation; $ECSA = C_{DL}/Cs$, where C_{DL} is the electrochemical double-layer capacitance and Cs is the capacitance of an atomically smooth planar surface.[1,2] In this work, Cs value of 40 μF cm^{-2} was employed.[3] Values of C_{DL} were calculated based on the following equation; $i = vC_{DL}$, where i is the double layer current measured by cyclic voltammograms at different scan rates (v) from 5 to 80 mV/s.

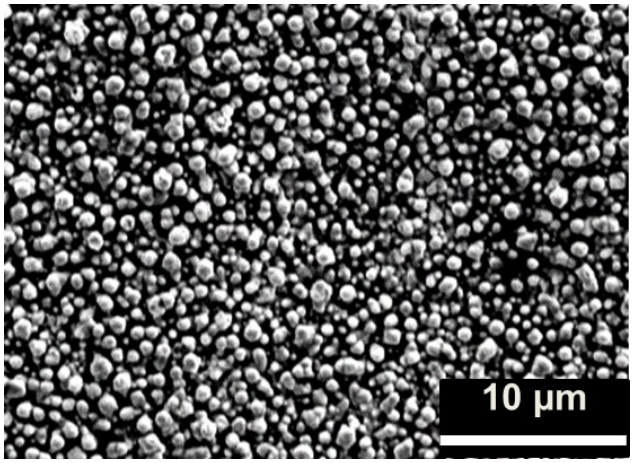

Fig. S1. Surface images of nodular type Cu substrate

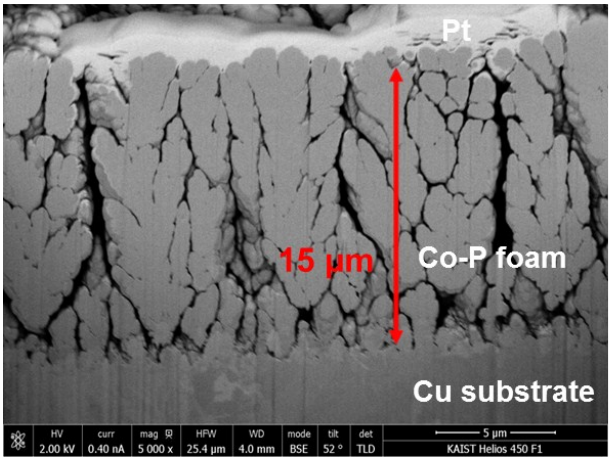

Fig. S2. Cross sectional SEM image of the Co-P foam.

.

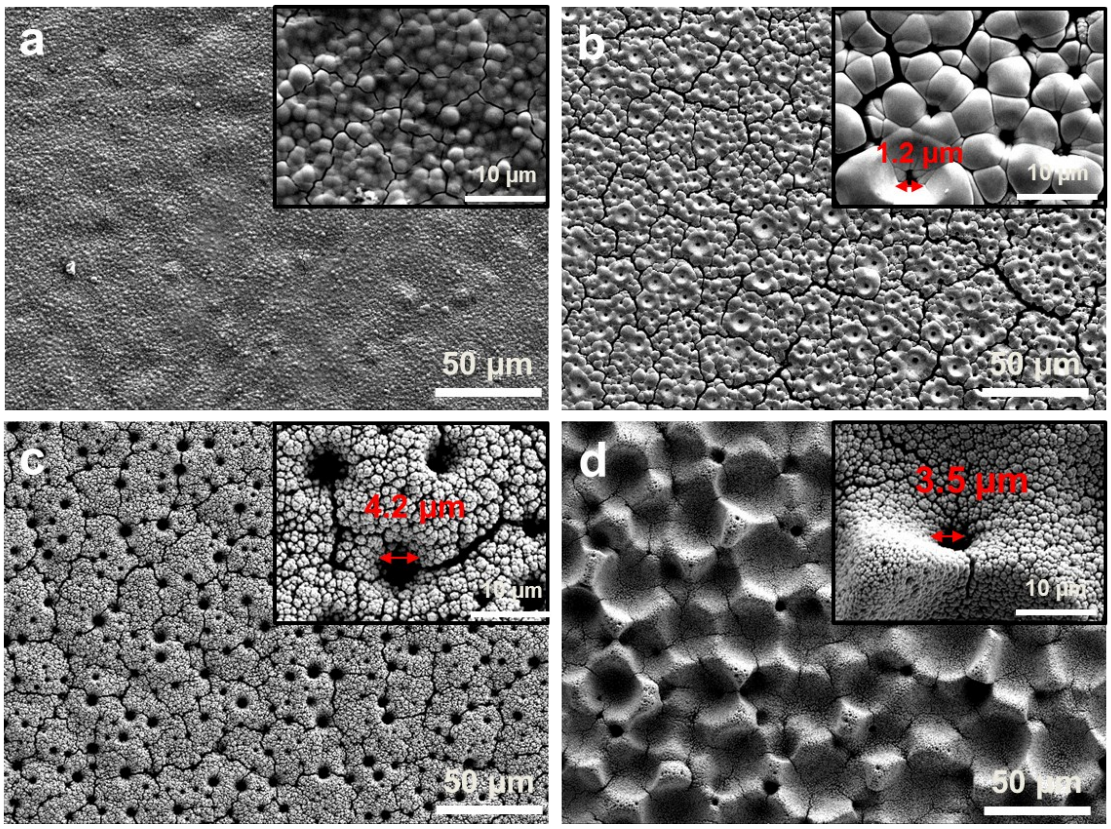

Fig. S3. SEM images of the Co-P catalysts electroplated at cathodic current densites of (a) 0.5, (b) 1, (c) 5 and (d) 9 A/cm^2.

Figure S3 shows the surface morphology of the Co-P catalysts electrodeposited on a Cu substrate at various cathodic current densities from 0.5 to 9 A/cm^2 for 10 s. For the Co-P sample electrodeposited at 0.5 A/cm^2 (Fig. S3a), spherical shaped crystals were formed smoothly. Micro cracks were observed in the film, indicating high residual stress was induced in the film by hydrogen evolution during the electrodeposition. With increasing cathodic current density to 1 A/cm^2 (Fig. S3b), macro pores in diameter of 1.2 μm were formed in the Co-P film. Small spherical particles were agglomerated and micro cracks were clearly observed even low magnification of SEM image due to the higher overpotential and faster hydrogen evolution than at 0.5 A/cm^2. With increasing current density to 3 A/cm^2, their

pore size was increased to 6 µm (Fig. 1b,c). For Co-P electrodeposited at 3 A/cm^2, the pore size and porosity were the highest among the prepared samples. It should be noted that as the cathodic current density was further increased to 5 (Fig. S3c) and 9 A/cm^2 (Fig. S3d), pore size in the Co-P structure remarkably decreased. For Co-P electrodeposited at 9 A/cm^2, pore size was approximately 3.5 µm.

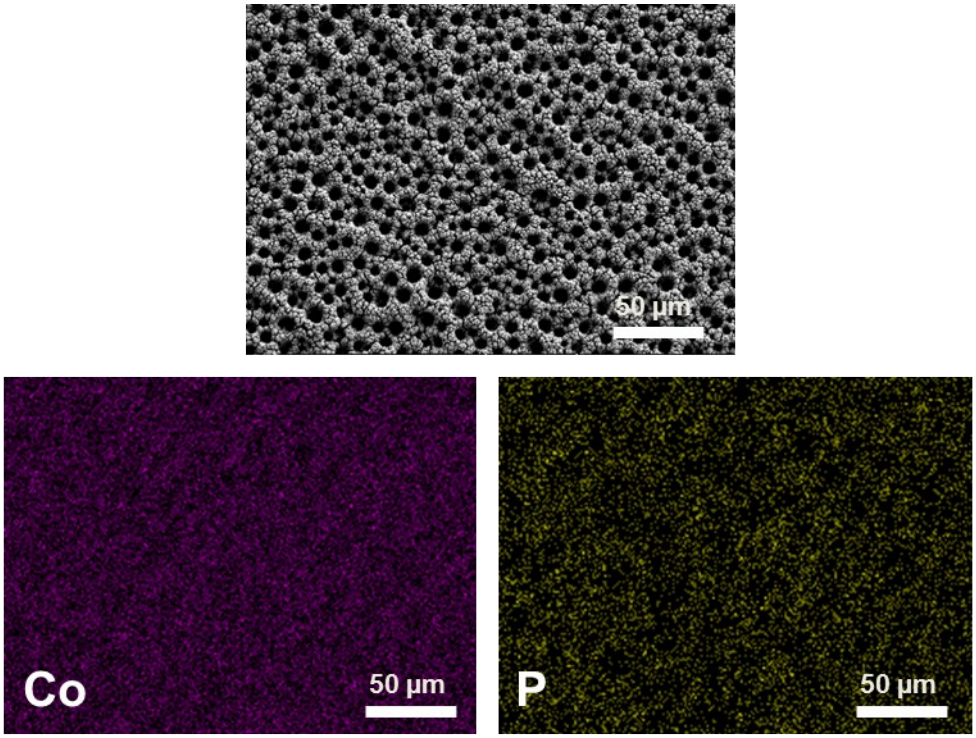

Fig. S4. (a) SEM image for the Co-P foam electrodeposited at 3 A/cm^2 and atomic mapping images of (b) Co and (c) P in the Co-P foam.

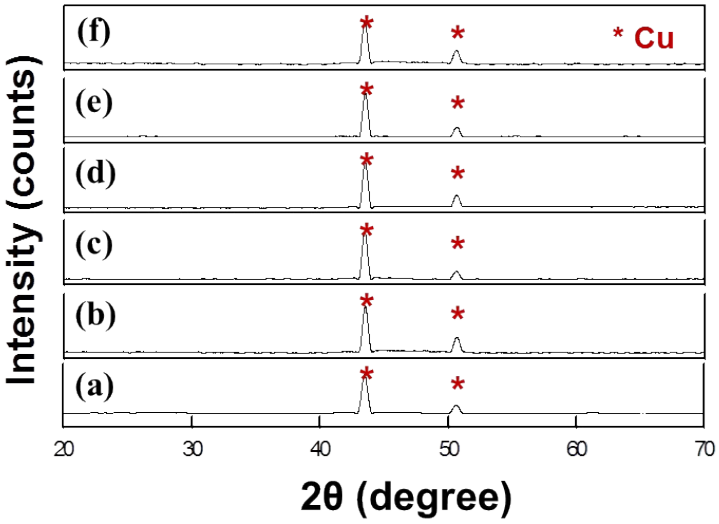

Fig. S5. XRD results of Co-P catalysts electrodeposited at current densities of (a) 0.5, (b) 1, (c) 3, (d) 5, (e) 9 A/cm^2 and (f) Co-P film.

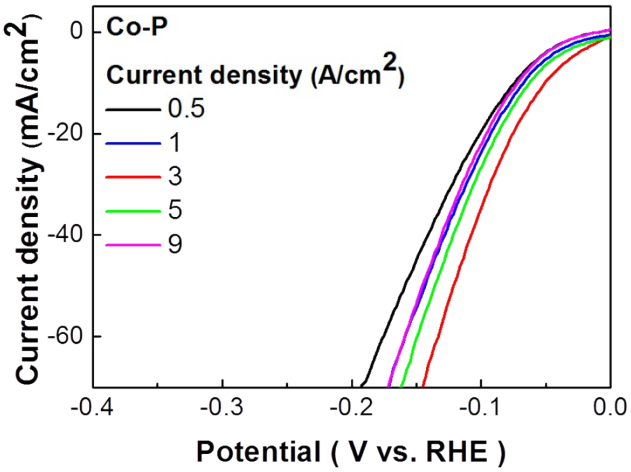

Fig. S6. HER activities for Co-P catalysts electrodeposited at current densities of 0.5, 1, 3, 5, and 9 A/cm^2 measured at 1 mV/s in H_2 saturated 0.5 M H_2SO_4 solution.

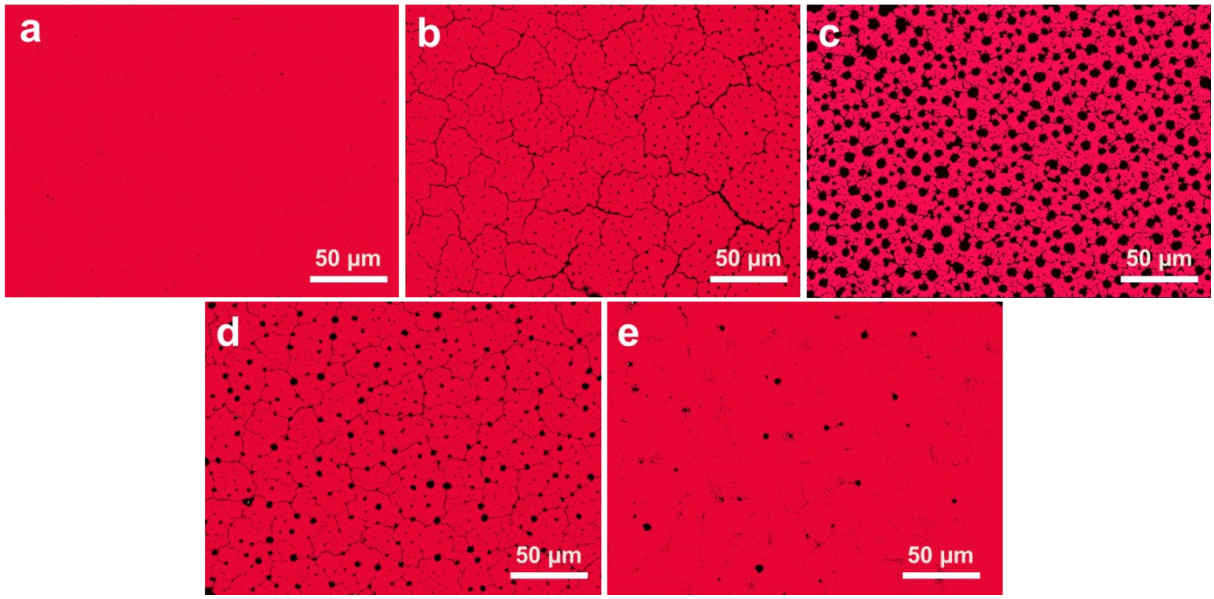

Fig. S7. Image analysis of Co-P catalysts electrodeposited at current densities of (a) 0.5, (b) 1, (c) 3, (d) 5, and (e) 9 A/cm^2.

Table S1. Porosity of Co-P catalysts electrodeposited at current densities of (a) 0.5, (b) 1, (c) 3, (d) 5, and (e) 9 A/cm^2.

Electrodeposition conditions of Co-P catalysts (mA/cm^2)	**Porosity (pore area/whole area, %)**
0.5	0.276
1	0.58
3	13.8
5	2.51
9	0.36

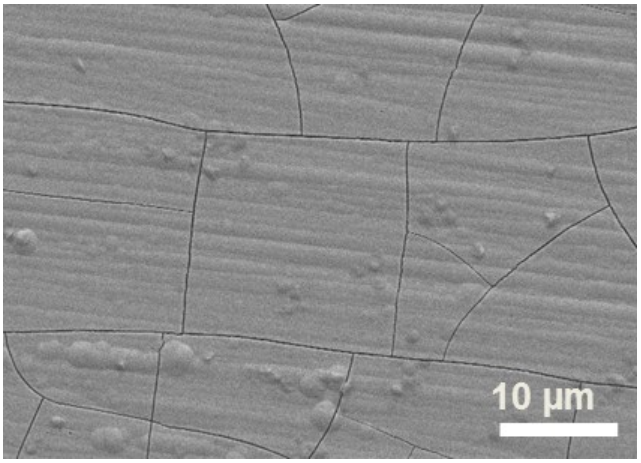

Fig. S8. Surface images of the Co-P film electrodeposited at 50 mA/cm^2.

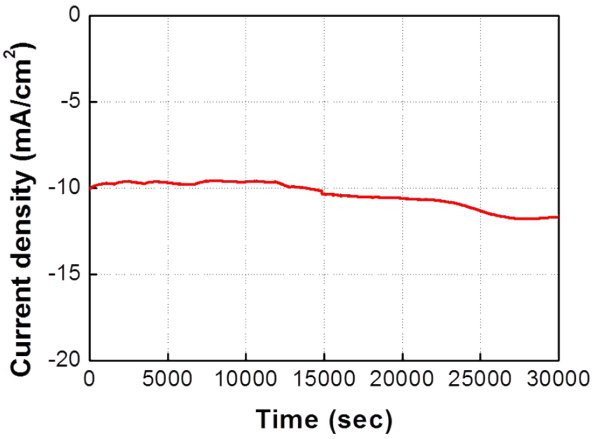

Fig. S9. Chronoamperometric responses (i–t) at an overpotential of 50 mV (η @ 10 mA/cm^2) in H_2-saturated 0.5 M H_2SO_4 solution.

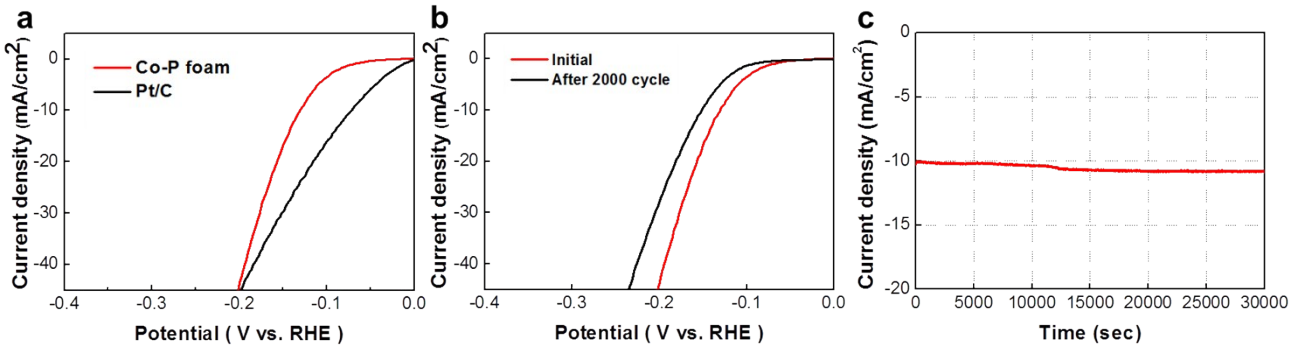

Fig. S10. (a) HER activities, (b) durability test of Co-P foam and Pt/C and (c) chronoamperometric responses (i–t) of the Co-P foam at an overpotential of 131 mV (η @ 10 mA/cm^2) in H_2-saturated 1 M KOH solution.

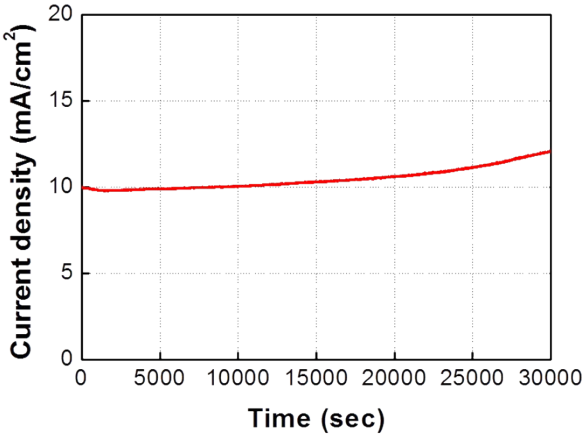

Fig. S11. Chronoamperometric responses (i–t) of the Co-P foam at at overpotential of 300 mV (η @ 10 mA/cm^2) mV in O_2-saturated 1 M KOH solution.

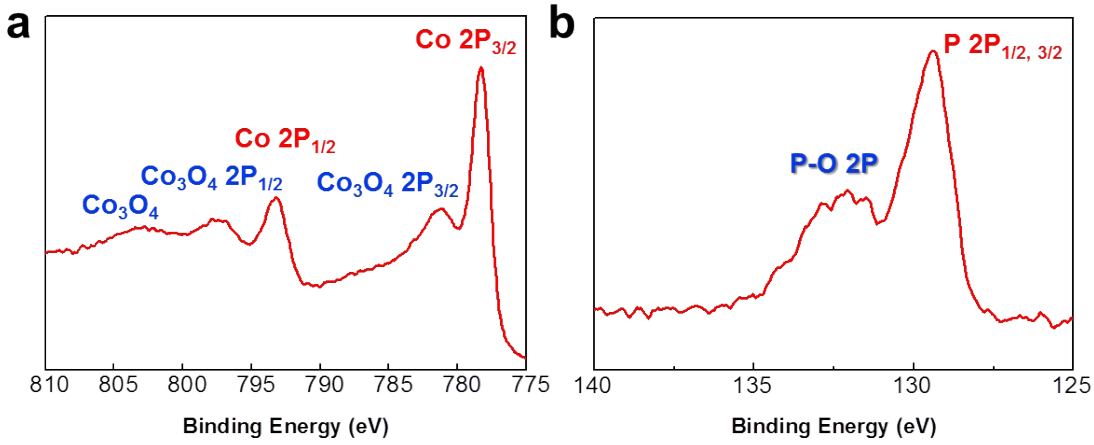

Fig. S12. XPS results of (a) Co 2p and (b) P 2p peaks of as prepared Co-P foam and that of Co-P foam after HER test.

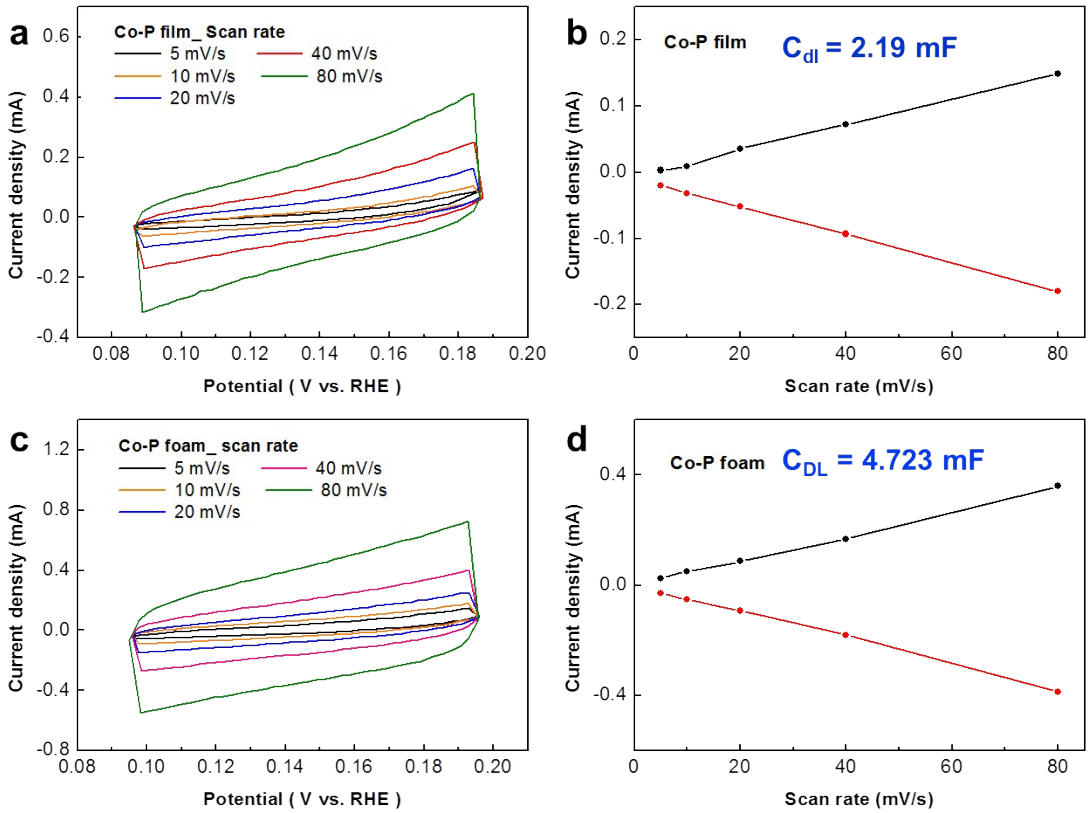

Fig. S13. Cyclic voltammograms measured at scan rates from 5 to 80 mV/s and corresponding *j vs.* scan rates plots for (a, b) the Co-P foam and (c, d) the Co-P film.

Table S2. HER activity Co-P catalysts in acidic media.[4-13]

Catalyst	**η_{10} (mV)**	**Electrolyte Conc. (H_2SO_4)**
Co-P foam (this work)	**50**	**0.5 M**
CoP[4]	67	0.5 M
CoP[5]	90	0.5 M
CoP[6]	48	0.5 M
CoP[7]	75	0.5 M
CoP/RGO[8]	270	0.5 M
CoP/mesoporous carbon[9]	112	0.5 M
CoP nanotubes[10]	129	0.5 M
Co_2P nanorods[11]	134	0.5 M
CoP[12]	98	0.5 M
CoP/CNT[13]	122	0.5 M

Table S3. OER activity of Co-P catalysts in alkaline media.[14-24]

Materials	**η_{10}(mV)**	**Electrolyte Conc. (KOH)**
Co-P foam (this work)	**300 mV**	**1 M**
Iron doped NiO[14]	297 mV	1 M
NiO/CNT[15]	350 mV	1 M
Ni_2P[16]	290 mV	1 M
Co-P film[17]	345 mV	1 M
NiCo LDH[18]	367 mV	1 M
CoCo LDH[19]	393 mV	1 M
Co3O4/rm-GO[20]	310 mV	1 M
CoxOy/NC[21]	430 mV	1 M
CoMn LDH[22]	324 mV	1 M
NiFeOx film[23]	350 mV	1 M
CoO/NG[24]	340 mV	1 M

Reference

1 Y. Yang, H. Fei, G. Ruan, J. M. Tour, Adv. Mater., 2015, 27, 3175-3180.

2 S. Trasatti, O. A. Petrii, Pure Appl. Chem., 1991, 63, 711-734.

3 J. D. Benck, Z. Chen, L. Y. Kuritzky, A. J. Forman, T. F. Jaramillo, ACS Catalysis, 2012, 2, 1916-1923.

4 J. Tian, Q. Liu, A.M. Asiri, X. Sun, J. Am. Chem. Soc., 2014, 136, 7587-7590.

5 Z. Pu, Q. Liu, P. Jiang, A.M. Asiri, A.Y. Obaid, X. Sun, Chem. Mater., 2014, **26**, 4326-4329.

6 Q. Li, Z. Xing, A.M. Asiri, P. Jiang, X. Sun, Int. J. Hydrogen Energy, 2014, **39**, 16806-16811.

7 E.J. Popczun, C.G. Read, C.W. Roske, N.S. Lewis, R.E. Schaak, Angew. Chem. Int. Ed. 2014, **53**, 5427-5430.

8 L. Ma, X. Shen, H. Zhou, G. Zhu, Z. Ji, K. Chen, J. Mater. Chem. A 2015, **3**, 5337-5343.

9 M. Li, X. Liu, Y. Xiong, X. Bo, Y. Zhang, C. Han, L. Guo, J. Mater. Chem. A, 2015, **3**, 4255-4264.

10 H. Du, Q. Liu, N. Cheng, A.M. Asiri, X. Sun, C.M. Li, J. Mater. Chem. A, 2014, **2**, 14812-14812.

11 Z. Huang, Z. Chen, Z. Chen, C. Lv, M.G. Humphrey, C. Zhang, Nano Energy, 2014, **9**, 373-382.

12 E. Popczun, C. Roske, C. Read, J.C. Crompton, J. McEnaney, J. Callejas, N. Lewis, R. Schaak, J. Mater. Chem. A, 2015, **3**, 5420-5425.

13 Q. Liu, J. Tian, W. Cui, P. Jiang, N. Cheng, A.M. Asiri, X. Sun, Angew. Chem. Int. Ed. 2014, **53**, 6710-6714.

14 K. Fominykh, P. Chernev, I. Zaharieva, J. Sicklinger, G. Stefanic, M. blinger, A. Mu¨ ller, A. Pokharel, S. Bo¨ cklein, C. Scheu,T. Bein, D. Fattakhova-Rohlfing, ACS Nano, 2015, **9**, 5180-5188.

15 N. Andersen, A. Serov, P. Atanassov, Applied Catalysis B, 2015, **163**, 623-627.

16 L. A. Stern, L. Feng, F. Song, X. Hu, Energy & Environment Science, 2015, **8**, 2347-2351.

17 Y.Yang, H. Fei, G. Ruan, J. M. Tour, Adv. Mater., 2015, **27**, 3175-3180.

18 H. Liang, F. Meng, M. Cabán-Acevedo, L. Li, A. Forticaux, L. Xiu, Z. Wang, S. Jin, Nano Lett., 2015, **15**, 1421-1427.

19 F. Song, X. Hu1, Nat. Commun., 2014, **5**, 4477-4485.

20 Y. Liang, Y. Li, H. Wang, J. Zhou, J.Wang, T. Regier, H. Dai, Nat. Mater., 2011, **10**, 780-786.

21 J. Masa, W. Xia, I. Sinev, A. Zhao, Z. Sun, S. Gr_tzke, P. Weide, M. Muhler, W. Schuhmann, Angew. Chem. Int. Ed., 2014, **53**, 8508-8512.

22 F. Song, X. Hu, J. Am. Chem. Soc., 2014, **136**, 16481-16484.

23 Charles C. L. McCrory, Suho Jung, Jonas C. Peters, Thomas F. Jaramillo, J. Am. Chem. Soc., 2013, **135**, 16977-16987.

24 S. Mao, Z. Wen, T. Huang, Y. Houa, J. Chen, Energy Environ. Sci., 2014, **7**, 609-616.